

# Exploding chemical gardens: a phase-change clock reaction

Yang Ding<sup>1</sup>, Carlos M. Gutiérrez-Ariza<sup>2</sup>, C. Ignacio Sainz-Díaz<sup>2</sup>,  
Julyan H. E. Cartwright<sup>2,3</sup>, Silvana S. S. Cardoso<sup>1\*</sup>

<sup>1</sup>Department of Chemical Engineering and Biotechnology, University of Cambridge,  
Cambridge, UK,

<sup>2</sup>Instituto Andaluz de Ciencias de la Tierra, CSIC–Universidad de Granada,  
E-18100 Armilla, Granada, Spain

<sup>3</sup>Instituto Carlos I de Física Teórica y Computacional, Universidad de Granada,  
E-18071 Granada, Spain

\*Corresponding author

## Abstract

Chemical gardens and clock reactions are two of the best known demonstration reactions in chemistry. Until now these have been separate categories. We have discovered that a chemical garden confined to two dimensions is a clock reaction involving a phase change, so that after a reproducible and controllable induction period it explodes.

**Keywords:** Chemical gardens · clock reactions · explosions · phase-change · chemobrionics

Many a youngster has become a chemist after the excitement of seeing for the first time — or even better, performing — one of the classic classroom experiments. Chemical gardens and clock reactions are two of these classic demonstration experiments that until now have been seen as entirely separate categories of reaction. But we have found that if one constrains a chemical garden to grow in two dimensions, within certain parameter ranges there is an induction time followed after many minutes by an explosion of the garden. This, then, is a version of the chemical garden that is also a chemical clock.

Chemical gardens, first described centuries ago by Glauber at the very beginnings of chemistry<sup>1</sup>, are the precipitation reactions of the cations of many metal salts with solutions of anions such as silicate, phosphate, carbonate and many more<sup>2</sup>. The particularity of these precipitates is that the solid formed has the right physical properties of cohesiveness and porosity so that it forms a semipermeable membrane, a partial barrier that is an impediment to some species and not to others. Reaction continues through the membrane to form a vesicle around the initial salt, and different ionic strengths on either side of this barrier lead to a movement of water under osmosis that may lead the membrane to rupture under osmotic pressure, on which buoyant fluid flows out. Further reaction at the interface of this plume with the surrounding fluid leads to the formation of a tube that templates the plume<sup>3:4</sup>. Chemical reaction plus fluid dynamics and osmosis together constitute an osmotic pump that produces in the classic chemical garden a series of tubular and vesicular forms that, seeming biotic, are dubbed a chemical garden. Recently such classical chemical gardens have been shown to be one of a series of phenomena linked by the formation of a self-assembled precipitate membrane and the field has been termed chemobrionics<sup>2</sup>. Applications include tubular structure formation in corrosion<sup>5</sup>, cement hydration<sup>6</sup>, polyoxometalates<sup>7</sup>, and the origin of life at submarine hydrothermal vents<sup>8</sup>.

Clock reactions arise from nonlinear chemical kinetics, and as such are linked to nonequilibrium processes, to nonlinear dynamical systems, to oscillations and to chaos<sup>9:10</sup>. The precise definition of a chemical clock is a matter of debate. Some have argued for a definition that restricts a clock reaction to an abrupt increase in the concentration of one or more products owing to the total consumption of a limiting reagent<sup>11</sup>, while others argue that it is not the details of the kinetics but the phenomenology that is important<sup>12</sup>. Yet others have equated clock reactions to oscillations<sup>13:14</sup>. But it is inarguable that the classic clock reactions are timers: they have a induction period that may be very long followed by a sharp change — often a colour change — at a given moment, and this induction time can be controlled and predicted by altering the quantities of reagents. Examples in gaseous combustion have noted the dependence of the induction time before explosion on the transport rates of chemicals and heat<sup>15:16</sup>. In the case of our scenario, the concept of a chemical clock is based upon the chemical-garden reaction acting as a timer whose period we can control. Here we describe and analyse the clock-reaction explosion of a chemical garden when confined to two dimensions.

Figure 1a shows the membrane growing at the interface between the inner solution containing the cation  $\text{Co}^{2+}$ , from the dissolving pellet, and the outer so-

lution of anion  $\text{SiO}_3^{2-}$ , according to the reaction



Moreover,  $\text{Co}^{2+}$  cations combine also with hydroxyl anions, forming cobalt hydroxides. Three zones delimited by the membrane can be distinguished: a central zone with a pink colour from the dissolving pellet, an intermediate zone with a clear colour; and the external zone with a fuchsia colour; the latter composes the membrane, which contains precipitated  $\text{CoSiO}_3$ . An ESEM micrograph of a segment of this membrane is also shown (Figure 1a). Energy-dispersive X-ray (EDX) analysis with an artificial-colour mapping of the distribution of Si (shown in red) and Co (blue) is displayed in Figure 1c and indicates that the smoother interior region of the membrane to the left is richer in silicon than the more rugged exterior surface to the right, which is mainly cobalt. The presence of this cation in the membrane surface could be owing to the distribution of cobalt after the explosion. An EDX mapping of the chemical composition of another region of the  $\text{CoSiO}_3$  membrane shows the distribution of Cl (green), Si (red) and Co (blue) (Figure 1d). The Cl is chloride anions coming from the initial seed; Si is silicate and Co the cobalt cation, probably in form of cobalt oxide/hydroxide. This concentration gradient is similar to that found in 3D chemical gardens<sup>17;18</sup>. Raman spectra of these samples (Figure 1b) show the presence of cobalt oxides with bands at 201 and 248  $\text{cm}^{-1}$ , which can be assigned to cobalt hydroxides and cobalt oxide. The intense band at 3400  $\text{cm}^{-1}$  can be assigned to the stretching vibration of the O-H bonds of hydroxides and molecules of water of crystallization. The band that appears at 1618  $\text{cm}^{-1}$  can be assigned to the bending vibrations of the molecules of water of crystallization<sup>19</sup>. The ESEM micrographs are of dried samples; although the drying and vacuum in the ESEM chamber produce macroscopic cracks, the microscopic morphology is not altered by the drying procedure<sup>18</sup>, and the drying process is at a low temperature of 25 – 40 °C, so that the cobalt hydroxides cannot dehydrate to oxides.

This membrane is initially impermeable to both the cobalt and silicate ions, but permeable to water, so that an osmotic pressure develops across it. The gradient of osmotic pressure drives water from the exterior environment into the cell enclosed by the membrane, thereby increasing the internal pressure. This increase in pressure, in turn, opens small cracks in the membrane and pumps the aqueous solution of cobalt outwards through these. A dual permeability membrane therefore develops: the chemistry controls the low permeability of the inflow regions, while the internal pressure and solid mechanics of the membrane control the higher permeability in the outflow regions. Figure 2 shows the trajectories of

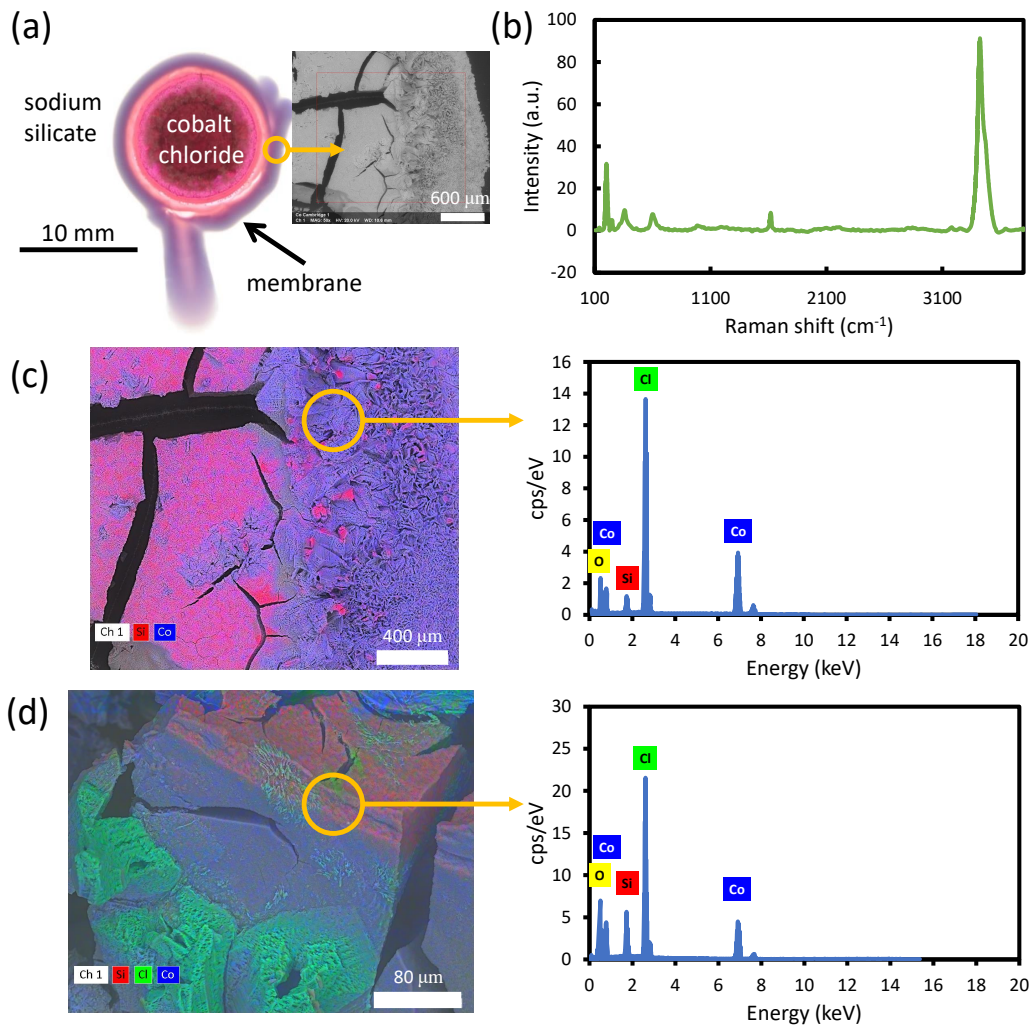


Figure 1: (a) Plan view of a precipitate membrane formed at a silicate concentration of 0.275 M and ESEM micrograph of a segment of the membrane. (b) Raman spectrum of one point of this sample. (c) ESEM micrograph of a segment of the circular membrane with false-colour EDX mapping of chemical composition of Si (red) and Co (blue) and the EDX spectrum at one point. (d) EDX mapping of an another part of the membrane with Cl (green), Si (red), and Co (blue) together with the EDX spectrum at one point.

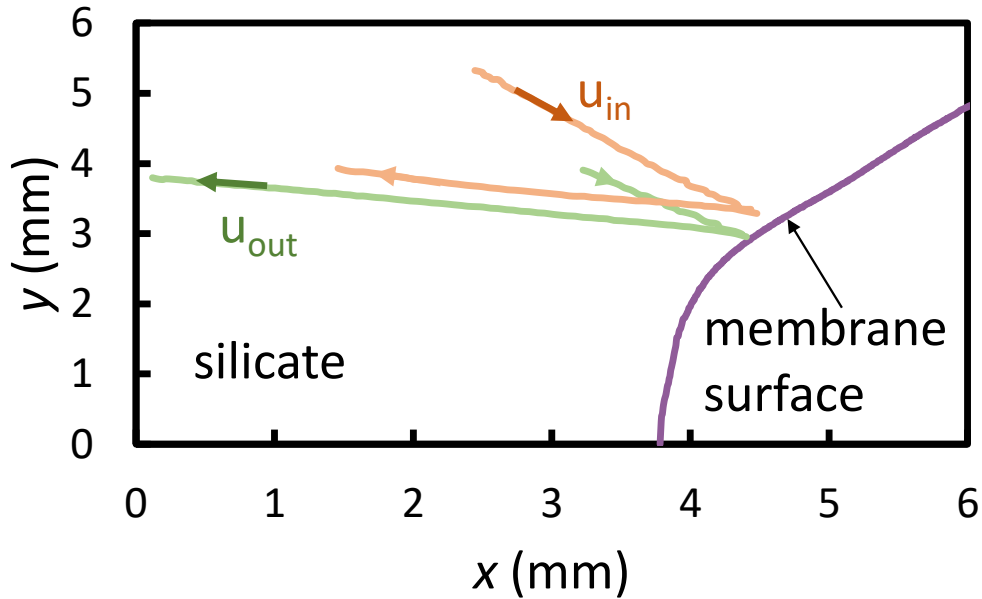


Figure 2: Measured trajectories of two seed particles near the membrane surface, at a silicate concentration of 0.275 M. The outside silicate solution flows towards the membrane with speed  $u_{in}$  driven by the osmotic pressure. Accumulation of water inside the cell builds up the internal pressure, which forces cobalt solution out of the membrane at speed  $u_{out}$ .

two seed particles as they move towards and away from the membrane surface. In all experiments, the outward flow decreases with time and the chemical garden ultimately explodes. Figure 3a depicts a sequence of photographs of an explosion for a concentration of silicate of 0.3 M. Figure 3a shows a section of the approximately circular inner-surface of the membrane, which then ruptures and allows the ejection of the inner cobalt solution. The ejected fluid subsequently oscillates inward and outward in several cycles, Figure 3b, while new solid precipitates at the interface with the external silicate solution. A well-defined steady finger of cobalt solution is seen at the end of the sequence. Such explosion of the chemical garden occurs at a reproducible time, which depends of the concentration of the silicate solution.

The evolution of the concentration of product at the interface between the two fluids,  $c$ , the pressure inside the cell enclosed by the membrane,  $p$ , and the

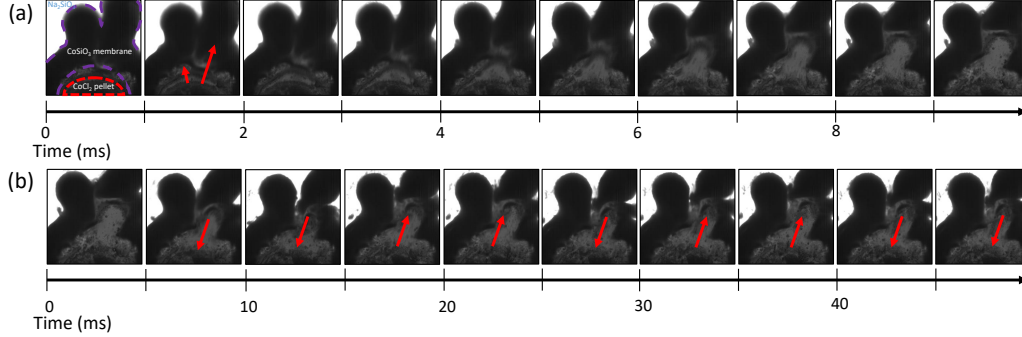


Figure 3: Sequence of photographs showing the rupture of the membrane and the ejection of cobalt solution, for a concentration of silicate of 0.30 M (oscillatory case). The rupture of the membrane is accompanied by the formation of a finger of cobalt solution (c), which oscillates to and from the membrane (d). Field of view:  $12.55 \times 12.55 \text{ mm}^2$ .

thickness of the membrane  $L_m$  can be written as

$$\frac{dc}{dt} = \left( u_{in} \frac{c_{Si}}{L_r} - u_{out} \frac{c}{R} \right) H[u_{out}], \quad (2a)$$

$$\frac{dp}{dt} = \gamma (u_{in} A_{in} - u_{out} A_{out}), \quad (2b)$$

$$\frac{dL_m}{dt} = \frac{MR}{\rho_s} \left( -\frac{dc}{dt} + \frac{u_{in} c_{Si}}{L_r} \right) H[u_{out}]. \quad (2c)$$

Here,  $c_{Si}$  is the concentration of the silicate solution,  $p_o$  is the osmotic pressure, and  $u_{in}$  and  $u_{out}$  are the radial speeds of external fluid towards the membrane and of the internal fluid at the outer edge of the membrane, respectively. As the internal fluid exits the membrane, it forms small fingers on the scale of the pore radii  $R$ . Reaction occurs on the surface of these fingers over a length scale  $L_r$ . The Heaviside step function  $H[u_{out}]$  ensures the product is only formed when there is outflow of cobalt ions. The deformation of the thin cylindrical membrane of thickness  $L_m$  is governed by the coefficient  $\gamma = (\partial p / \partial V)_T = 2L_m E / (R_p V_p)$ , where  $R_p$  and  $V_p$  are the radius and volume of the solid pellet, while  $E$  denotes Young's modulus for the membrane material. The surface areas for inward osmotic flow  $A_{in}$  and for the outward flow  $A_{out}$  are assumed constant. Thus, the

first equation describes a balance between the supply of silicate ion for reaction and product buildup, and the spreading of product owing to outflow. The second equation quantifies the change in pressure owing to the change in the volume of fluid inside the cell enclosed by the membrane. The third equation relates the rate of growth of the membrane to the difference between the flux of silicate ions towards the membrane and the rate of accumulation of the solid at its surface.

The radial osmotic and outward speeds are given by<sup>20;21;22</sup>

$$u_{in} = \frac{k_{in} p_o - p}{\mu L_m}, \quad (3a)$$

$$u_{out} = \frac{k_{out} p}{\mu L_m} \left(1 - \frac{c}{c^*}\right) H\left[1 - \frac{c}{c^*}\right]. \quad (3b)$$

Here,  $k_{in}$  and  $k_{out}$  are the permeabilities of the membrane<sup>23</sup> in the regions of inflow and outflow, respectively, while  $\mu$  is the viscosity of the fluids without product. As the concentration of product increases at the interface of the inner and outer fluids, the speed of the outflowing fingers decreases; the motion ceases above the critical product concentration  $c^*$ . This form of dependence of the speed on concentration was first proposed by<sup>24</sup> for the growth of a precipitate filament. We introduce the Heaviside step function  $H[1 - c/c^*]$  to ensure that  $c \leq c^*$  and  $u_{out} \geq 0$ .

Substituting the speed relations (3) into the governing equations (2) and non-dimensionalizing (see Supporting Information) shows that the behaviour of the system depends only on two non-dimensional groups:  $N = p_o k_{in} A_{in} V R_p / (2EL_s k_{out} A_{out}^2 R)$  represents the ratio of the timescales for outflow and for osmotic pumping;  $M = N[(c_{Si} A_{out} R) / (c^* A_{in} L_r)]$  represents the ratio of the timescales for outflow and for accumulation of solid. In the simplified limit of  $A_{out} \sim A_{in}$  and  $R/L_r \sim 1$ , then  $M \approx N c_{Si} / c^*$ . Our previous study of the frozen-time behaviour of the membrane, in which its growth was neglected, revealed the following properties:  $EA_{out} = 7.4 \times 10^{-3} \text{ Pa m}^2$ ,  $A_{in}/A_{out} = 0.98$  and  $R = 4.5 \times 10^{-4} \text{ m}$ . These properties are used below to determine the nonlinear time-dependent behaviour of the system.

In the laboratory, we have measured the pressure inside the pellet, but we cannot measure directly the concentration of solid at the reaction front on the outer surface of the membrane. We can however measure the surface area of the solid membrane  $S$ . We expect this surface area to grow following  $dS/dt \sim dL_m/dt \sim u_{out} c \sim -dc/dt + u_{in} c_{Si} / L_r$ . The last term here is approximately constant, so that any temporal oscillations in  $c$  will be reflected as oscillations in  $S$  too. Figure

4 depicts the evolution of the measured pressure, as well as the rate of change of the surface area of the solid membrane, in our experimental system for a range of concentrations of the silicate solution. Also shown are the corresponding predictions of our model S.1 for the pressure and concentration of product, using permeabilities of the membrane in the inflow and outflow regions within the measured range (see Table 1, Supporting Information). We can identify three regimes of behaviour, according to the early-time evolution. In the stable regime, 4a, the pressure and concentration of product remain low for some time, but later increase when the permeability of the membrane decreases. After the membrane closes, the pressure increases drastically leading to rupture. The measured and predicted pressure increases are in good agreement. The oscillatory case, 4b, exhibits initial oscillations for both pressure and concentration, followed by a sudden increase as the permeability of the membrane decreases. In both the stable and oscillatory cases, the concentration of product remains well below the threshold at which the outflow stops until the permeability decrease becomes significant. In contrast, in the unstable behaviour, 4c, the concentration grows fast initially, decreasing the flow out of the membrane, and inducing a rapid pressure increase. The decreasing permeability in the outflow regions as the membrane grows is presented in Figure 5 for all three regimes. The agreement between experiments and theory is good; in the oscillatory and unstable cases, the outflow permeability drops off slightly more rapidly than predicted, but given the minimal physical model considered here, the difference is acceptable. In all three regimes, the membrane ultimately blocks, inducing a rapid pressure increase and explosion of the membrane. However, the mechanisms leading to explosion are different. For low silicate concentrations, the decrease in permeability owing to closure of small pores during the membrane growth is crucial. For high silicate concentrations, the concentration of product at the outer surface of the membrane drives the increase in pressure and eventual rupture of the membrane; this mechanism is reflected in the more abrupt decrease of the permeability in the outflow regions. In the next section, we analyse these two limits of behaviour further.

As precipitation progresses, the exit pathways within the membrane get blocked. The external fluid continues to be pumped in osmotically, causing a rise in the internal pressure, and the eventual rupture of the membrane. We may derive the

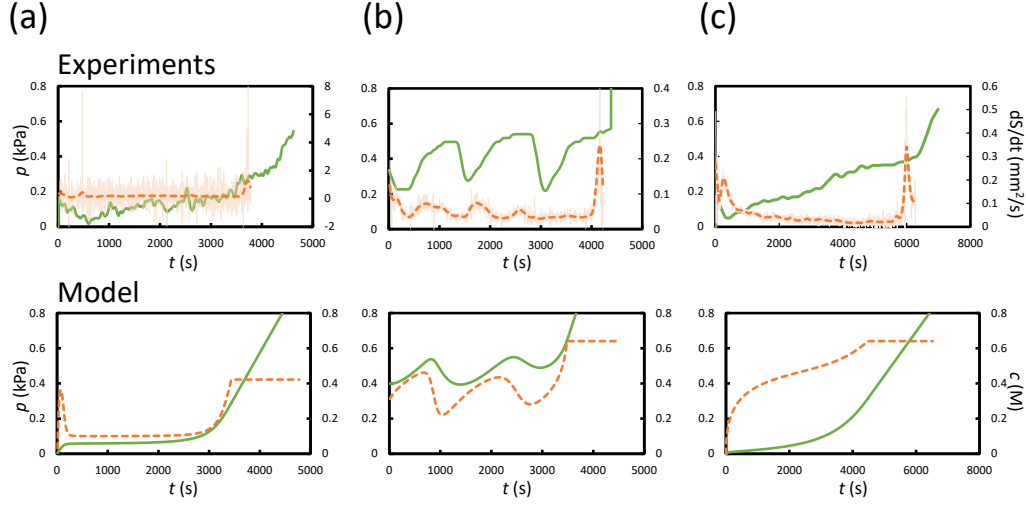


Figure 4: Comparison of experimental measurements (top) and theoretical predictions (bottom) for the membrane behaviour in the (a) stable, (b) oscillatory and (c) unstable regimes. Shown are the experimental pressure (solid line) and rate of increase of surface area of precipitate (dashed line), and the theoretical predictions of (2) for the pressure (solid line) and concentration of product (dashed line).

following asymptotic limits for the explosion time (see Supporting Information),

$$t_{e1} \approx \frac{\mu R_p V_p}{2EA_{out}k_{out0}} \left( \frac{G^{1/2} \sigma_c L_s}{p_s R_p N} + G \frac{N}{M} \right), \quad \text{for low } c_{Si} \quad (4a)$$

$$t_{e2} \approx \frac{\mu R_p V_p}{2EA_{out}k_{out0}} \left( \frac{\sigma_c L_s}{2p_s R_p N^2} + \frac{1}{4NM} \right), \quad \text{for high } c_{Si} \quad (4b)$$

where  $\sigma_c$  is the critical circumferential stress at which the membrane ruptures.

Figure 6a shows the ruptured membrane for varying concentration of the silicate solution. While at low silicate concentration, the ejection of cobalt solution following rupture is a localized event, at larger concentration the flow of cobalt is more diffuse, indicating the rupture of the membrane in several positions. The critical stress at which the membrane ruptures increases with the silicate solution concentration, as presented in Figure 6b. These measurements are consistent with observations of a flaky, fragile membrane at low concentrations and a more robust one at high concentrations. The measured and predicted explosion times as a function of silicate concentration are shown in Figure 6c. The numerical

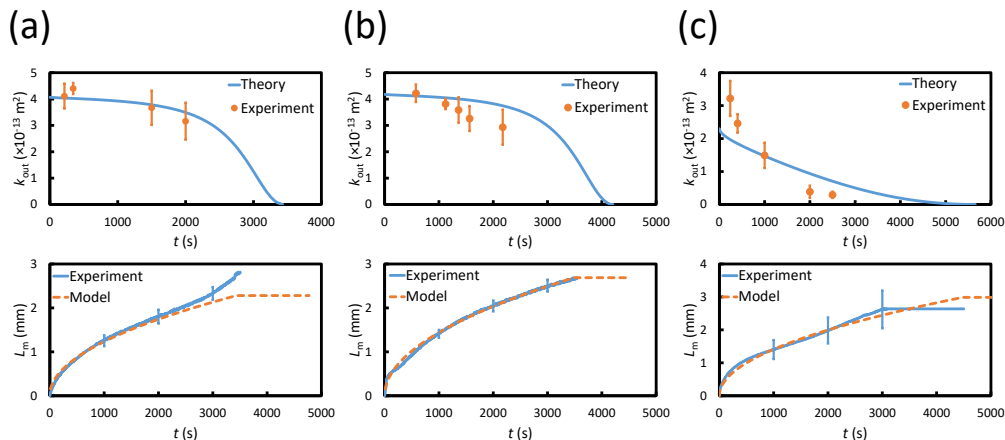


Figure 5: Evolution of the membrane permeability in the outflow regions (top) and membrane thickness (bottom) for example cases of (a) stable, (b) oscillatory and (c) unstable behaviours.

and asymptotic predictions are in excellent agreement with the measured explosion times, showing that the physical mechanisms leading to the explosion of the membrane have been well captured by the simple model. For increasing silicate concentration, the explosion time first decreases since the membrane cannot block in the limit of zero concentration, but then increases owing to an increase in the critical stress of the membrane. For higher silicate concentration, the solid on the outer surface of the membrane attains the critical concentration required to block the flow at earlier times, so the explosion time decreases.

Our description of this version of the chemical garden as a chemical clock begs the question of what a chemical clock is. The widest definition of a chemical clock would encompass any oscillatory reaction. For example, recently Goesten et al.<sup>14</sup> described what they termed a clock reaction in which a solidifying entity, a metal–organic framework, displays oscillations in crystal dimension and number. Similarly, McEwen et al.<sup>13</sup> described a clock reaction of oscillations on the surface of a catalyst. We see this definition of a chemical clock as too broad to be useful. On the other hand, we see as unduly restrictive the proposal of Lente et al.<sup>11</sup> that only reactions with a very particular kinetics whereby a given limiting reagent is used up to enable a subsequent rapid increase in the clock product should be considered as clock reactions. We argue that the definition of a chemical clock should neither be so restrictive that only one kinetic mechanism is possible nor

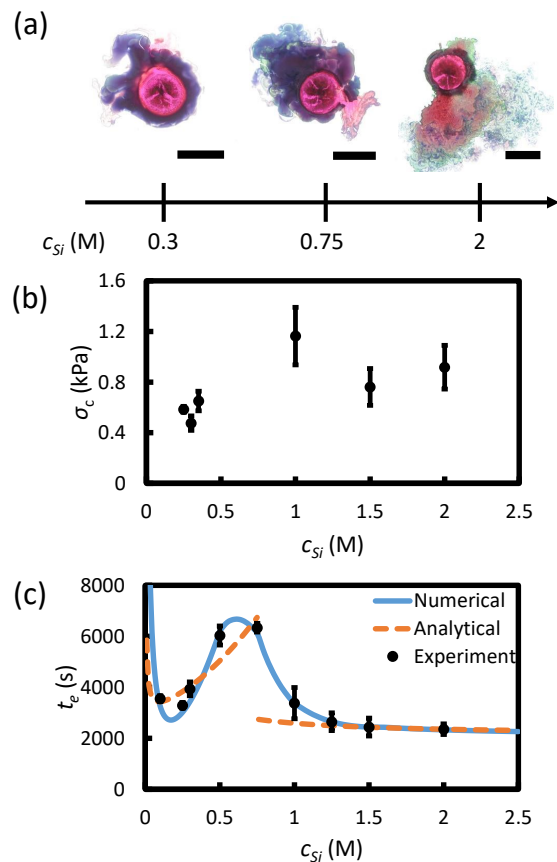


Figure 6: (a) Photographs of ruptured membrane for varying concentration of the silicate solution. Scale bars: 10 mm. (b) Measured circumferential stress on the membrane at the time of explosion. (c) Variation of the time to explosion with the concentration of the silicate solution. Experimental measurements are compared with the numerical prediction (2) (solid line) and the asymptotic solutions (4) (dashed lines).

so open that any oscillating reaction is sufficient, but should recognise that the classical idea of a chemical clock is that of a timer, which is what we have here.

Most clock reactions involve kinetics and chemical transport. In contrast, the chemical-garden clock reaction involves kinetics, chemical transport, and also solid mechanics: the membrane deformation. Chemical-garden reactions in gen-

eral have not previously been shown to have clock-reaction dynamics. However, cement hydration is a well known and commercially important precipitation reaction, and cement hydration is another example of chemobrionics closely linked to chemical gardens<sup>2</sup>. Interestingly, cement hydration has an induction period and this has been put in the context of clock reactions<sup>25</sup>. It is clearly of significance to seek to apply the present results to the cement case, with the idea of achieving a better understanding of the mechanisms of hydration acceleration and retardation that would have wide industrial applicability<sup>26</sup>.

Our clock keeps reasonable but not perfect time. According to Figure 6c the system is a better timer at higher and lower concentrations of silicate than at intermediate concentrations. Fluctuations in clock reaction dynamics have also been investigated, wherein chaotic and stochastic aspects — i.e., both non-linear behaviour and noise — of the dynamics can give rise to so-called crazy clocks where the lag time has a varying component<sup>27:28</sup>. We calculate two limits for the explosion time and plot them on the data in Figure 6c, and it is interesting to wonder about the jump between the two limits in the middle of the graph and its possible relationship with fluctuations in explosions times. In our case the trajectory escapes to infinity, but there might possibly be transient chaos, which would lead to a spread of explosion times for those concentrations. However, altering the initial conditions of the simulations shows that the results are quite robust; we did not see any difference in the explosion time when changing the initial condition of non-dimensional pressure from 0 to at least 10, and initial condition of non-dimensional concentration 0 to 0.4. Hence the experimental spread in explosion times at intermediate concentrations is likely to be a stochastic effect not present in our physical model.

The simple physical model presented here is capable of describing the emergent dynamical regimes observed in the experiments. The focus has been in reducing the multitude of physical and chemical processes in the self-assembling chemical-garden membrane to the interaction of osmotic flow and chemical reaction in the membrane. This is a beautiful example of active fluid dynamics, where the chemistry controls the flow, which in turn can lead to a physical explosion.

## References

- [1] J. R. Glauber, *Furni Novi Philosophici*, Amsterdam, **1646**.
- [2] L. M. Barge, S. S. S. Cardoso, J. H. E. Cartwright, G. J. T. Cooper, L. Cronin,

- A. De Wit, I. J. Doloboff, B. Escribano, R. E. Goldstein, F. Haudin, D. E. H. Jones, A. L. Mackay, J. Maselko, J. J. Pagano, J. Pantaleone, M. J. Russell, C. I. Sainz-Díaz, O. Steinbock, D. A. Stone, Y. Tanimoto, N. L. Thomas, *Chem. Rev.* **2015**, *115*, 8652–8703.
- [3] S. Thouvenel-Romans, O. Steinbock, *J. Amer. Chem. Soc.* **2003**, *125*, 4338–4341.
- [4] D. A. Stone, B. Lewellyn, J. C. Baygents, R. E. Goldstein, *Langmuir* **2005**, *21*, 10916–10919.
- [5] G. Butler, H. C. K. Ison, *Nature* **1958**, *182*, 1229.
- [6] D. D. Double, A. Hellowell, *Nature* **1976**, *261*, 486.
- [7] G. J. T. Cooper, A. G. Boulay, P. J. Kitson, C. Ritchie, C. J. Richmond, J. Thiel, D. Gabb, R. Eadie, D.-L. Long, L. Cronin, *J. Amer. Chem. Soc.* **2011**, *133*, 5947–5954.
- [8] A. J. Boyce, M. L. Coleman, M. J. Russell, *Nature* **1983**, *306*, 545.
- [9] P. Gray, S. K. Scott, *Chemical Oscillations and Instabilities: Non-Linear Chemical Kinetics*, Clarendon Press, **1990**.
- [10] J. A. Pojman, I. R. Epstein, *An Introduction to Nonlinear Chemical Dynamics: Oscillations, Waves, Patterns, and Chaos*, Oxford University Press, **1998**.
- [11] G. Lente, G. Bazsa, I. Fábián, *New J. Chem.* **2007**, *31*, 1707.
- [12] J. Billingham, D. J. Needham, *J. Eng. Math.* **1993**, *27*, 113–145.
- [13] J.-S. McEwen, P. Gaspard, T. V. de Bocarmé, N. Kruse, *Proc. Natl Acad. Sci. USA* **2009**, *106*, 3006–3010.
- [14] M. G. Goesten, M. F. de Lange, A. I. Olivos-Suarez, A. V. Bavykina, P. Serra-Crespo, C. Krywka, F. M. Bickelhaupt, F. Kapteijn, J. Gascon, *Nature Commun.* **2016**, *7*, 11832.
- [15] T.-Y. Liu, S. S. Cardoso, *Combustion and Flame* **2013**, *160*, 191 – 203.
- [16] F. Goncalves de Azevedo, J. F. Griffiths, S. S. S. Cardoso, *Phys. Chem. Chem. Phys.* **2013**, *15*, 16713–16724.

- [17] J. H. E. Cartwright, B. Escibano, C. I. Sainz-Díaz, *Langmuir* **2011**, *27*, 3286–3293.
- [18] J. H. E. Cartwright, B. Escibano, S. Khokhlov, C. I. Sainz-Díaz, *Phys. Chem. Chem. Phys.* **2011**, *13*, 1030–1036.
- [19] J. Yang, H. Liu, W. N. Martens, R. L. Frost, *J. Phys. Chem. C* **2010**, *114*, 111–119.
- [20] A. J. Staverman, *Rec. Trav. Chim. Pays-Bas* **1951**, *70*, 344.
- [21] O. Kedem, A. Katchalsky, *Biochim. Biophys. Acta* **1958**, *27*, 229.
- [22] S. S. S. Cardoso, J. H. E. Cartwright, *Roy. Soc. Open Sci.* **2014**, *1*, 140352.
- [23] D. Turcotte, G. Schubert, *Geodynamics*, Cambridge University Press, **2002**.
- [24] S. Wagatsuma, T. Higashi, Y. Sumino, A. Achiwa, *Phys. Rev. E* **2017**, *95*, 052220.
- [25] J. Billingham, D. J. Needham, *J. Chem. Soc. Faraday Trans.* **1993**, *89*, 3021–3028.
- [26] S. S. S. Cardoso, J. H. E. Cartwright, O. Steinbock, D. A. Stone, N. L. Thomas, *Struct. Chem.* **2017**, *28*, 33–37.
- [27] I. R. Epstein, *Nature* **1995**, *374*, 321–327.
- [28] L. Valkai, G. Cseko, A. K. Horváth, *Phys. Chem. Chem. Phys.* **2015**, *17*, 22187.

## Acknowledgements

JHEC and CISD acknowledge the financial support of the Spanish MINCINN projects FIS2016-77692-C2-2-P and PCIN-2017-098.

## Author contributions

All authors contributed in an integrated manner to this work.

## **Competing financial interests**

The authors declare no competing financial interests.